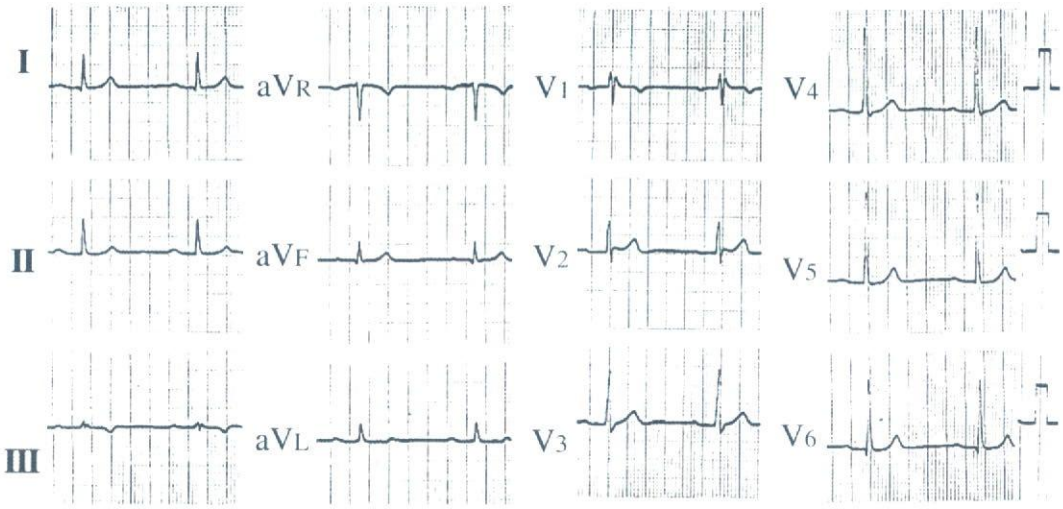

Fig 1. ECG prior to lithium administration shows first-degree atrioventricular block (PQ interval: 280 ms).

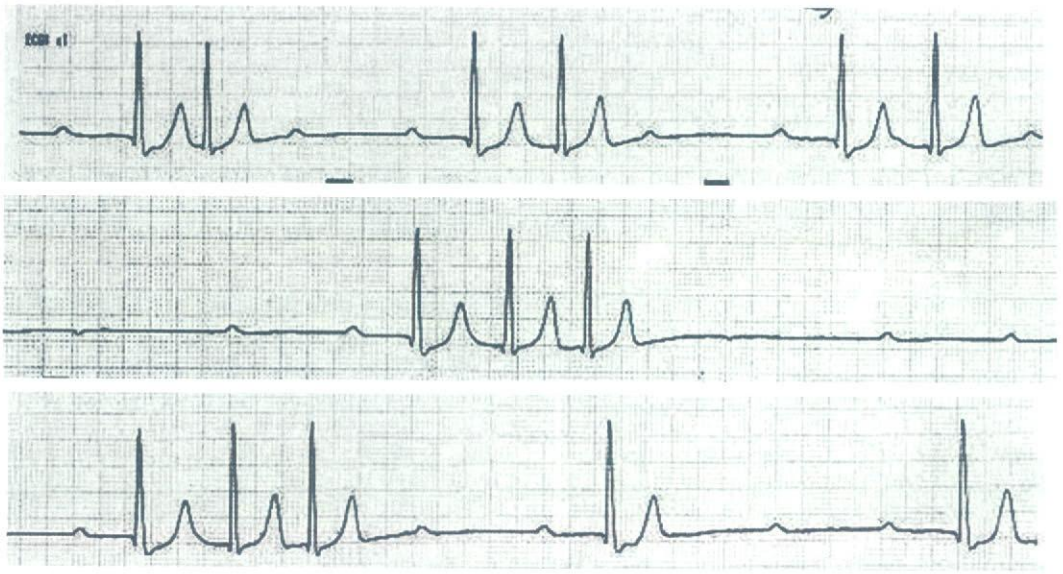

Fig 2. Monitoring record of the ECG at the first syncopal attack shows complete atrioventricular block (CAVB) (atrial rate during CAVB: 60–65 beats/min). The interval of the first QRS complex after atrioventricular (AV) block was 120 ms, and those of the second and third are less than 120 ms. Although the morphology of the first is slightly different from the others, these results reveal that the QRS complexes are supraventricular (SV) escaped beats. The first P-wave on the second line and the P-wave after SV escaped beats indicate SV escaped beats with AV block. The deficit of the P-wave from the sinus node between QRS complexes and the escaped beat means non-conducted normal sinus activity interfered with refractory periods after SV escaped beats. These results show no sinus node dysfunction at the first attack. Serum lithium concentration was below therapeutic range (0.3 mmol/L).

implanted after informed consent was given. Finally, the patient did well during the subsequent 2 months on a regimen of valproate alone and he was then discharged.

Discussion

This patient presented with 2 paroxysmal CAVB attacks during lithium therapy for manic disorder. Lithium, like sodium, enters the cardiac cells and ineffective removal causes intracellular replacement of potassium[1] Lithium decreases spontaneous depolarization of the sinus node and the conduction velocity in the AV and intraventricular conduction systems[2] Moreover, the reduced adrenergic response and interference with calcium influx in the pacing cells of the sinus node may be regarded as other possible effects[1,3]

Prolonged use and overdose of lithium have frequently been associated with cardiac side-effects, such as asymptomatic T-wave changes, SND, sinoatrial block, ventricular arrhythmias, and myocarditis[4,5] Although arrhythmia-related SND is a frequent complication of lithium treatment with or without intoxication, CAVB necessitating permanent pacemaker, as seen in this case, is very unusual[6–10]

This case presents several points of major interest.

At the start of ECG monitoring several minutes after the onset of both syncopal attacks, the rhythms preceding the onset were unknown. The interval of the first QRS complex after AV block was 120 ms, and those of the second and third were less than 120 ms. Although the QRS morphology of the

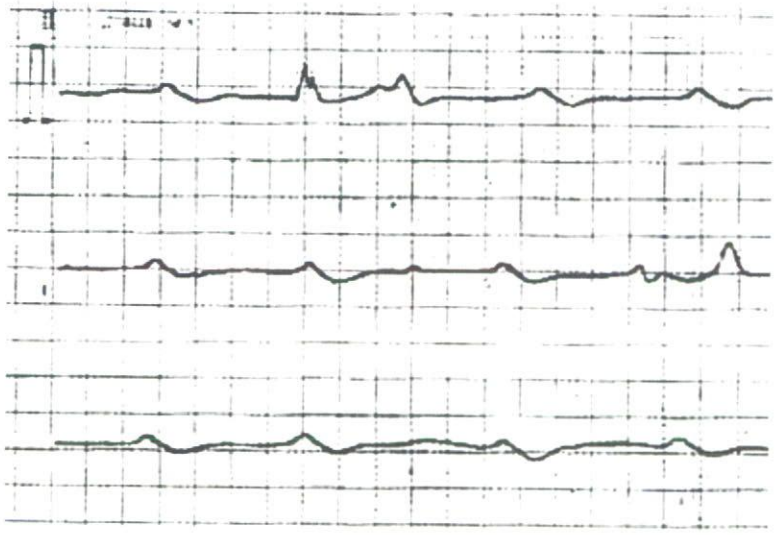

Fig 3. Monitoring report of the ECG at the second syncopal attack shows complete atrioventricular block. The atrial rate of 50–68 beats/min reveals slight sinus nodal dysfunction. Severe ventricular bradycardia can be seen. The serum lithium concentration was within the therapeutic range (0.85 mmol/L).

first attack was slightly different from the others, these results reveal that the QRS complexes might have been supraventricular (SV) escaped beats (Fig 2).

The first P-wave on the second line and the P-wave after the SV escaped beats indicate escaped beats with AV block. The deficit of the P-wave from the sinus node between QRS complexes and the escaped beat indicates non-conducted normal sinus activity interfered with the refractory periods after SV escaped beats. These results showed no SND at the first syncope attack (Fig 2).

Severe ventricular bradycardia with a slightly slow atrial rate was observed at the second syncope attack (Fig 3). Diurnal change of the PR interval and not worsened AV block related to the heart rate increase were observed. These results show that AH or BH block might have caused the first CAVB, including first-degree AV block before lithium administration, and HV block might have caused the second CAVB after lithium administration.

The 2 syncopal attacks were not related to the serum lithium level. The first attack occurred while the serum lithium level was below the therapeutic range, and the second occurred while it was within the therapeutic range.

With regard to the PP intervals at the first syncope, SND was not detected during complete AV block with no ventricular escaped beats. On the other hand, during lithium intoxication the patient had no cardiovascular signs with the exception of sinus bradycardia. The first attack might have resulted from the combination of lithium below the therapeutic range and carbamazepine, which can affect a preexisting mild AV conduction disturbance![11] The second attack occurred during treatment with lithium within the therapeutic range and valproate, with no cardiovascular effect. During lithium intoxication, additionally introduced levomepromazine, which has the cardiovascular side-effect of tachycardia[12] and therefore was not administered for the syncope attacks, could have prevented the onset of advanced AV block.

This case seems to indicate that AV block, and likewise SND, can occur with any dose of lithium, at any stage of the treatment. We did not perform an electrophysiological study of AV conduction and permanent pacemaker implantation just after the first syncope attack because of his unstable psychosomatic condition and the absence of a guarantor. We were permitted to perform only temporary pacing for resuscitation at both syncope attacks and permanent pacemaker implantation at the second attack. A head-up tilt test to rule out neurally mediated syncope (NMS) was also not conducted. Latent AV node disease or NMS, which might worsen following lithium treatment, cannot be excluded. Therefore, we could not sufficiently prove that lithium might have caused the 2 attacks of CAVB. Nevertheless, emergence of primary disease frequently requires medical treatment with minimal examinations that might have adverse effects on the cardiac conducting system.

In conclusion, lithium should be used with great caution, especially in patients with a conduction disturbance, and when there are additional psychotic medications that might decrease intracardiac conduction velocity. Moreover, in patients taking psychotropic agents that might cause bradyarrhythmia, the risk of unnecessary implantation of a permanent pacemaker should be kept in mind.

References

1. Singer I, Rotenberg D. Mechanism of lithium action. *N Engl J Med* 1973; **289:** 254–260.
2. Ricciutti MA, Lisi KR, Damato AN. A metabolic basis for the electrophysisologic effects of lithium. *Circulation* 1971; **44**(Suppl)**:** 217.
3. Roose SP, Nurnberger JI, Dunner DL, Blood DK, Fieve RR. Cardiac sinus node dysfunction during lithium treatment. *Am J Psychiatry* 1979; **136:** 804–806.
4. Tilkian T, Schroeder J, Kao J. The cardiovascular effects of litium in man. *Am J Med* 1989; **61:** 665–670.
5. Mitchell JE, Mackenzie TB. Cardiac effects of lithium therapy in man: A review. *J Clinical Psychiatry* 1982; **43:** 47–51.
6. Montalescot G, Levy Y, Farge D, Brochard L, Fantin B, Arnoux C, et al. Lithium causing a serious sinus-node dysfunction at therapeutic doses. *Clin Cardiol* 1984; **7:** 617–620.
7. Weintraub M, Hes JP, Rotemensch HH, Soferman G, Liron M. Extreme sinus bradycardia associated with lithium therapy. *Isr J Med Sci* 1983; **19:** 353–355.
8. Ricconi N, Roni P, Batrtolomei C. Lithium-induced sinus node dysfunction. *Acta Cardiol* 1983; **38:** 133–138.
9. Hussain KM, Konstandy G, Kurz L, Pachter BR. Hemodynamic, electrocardiographic, metabolic, and hematologic abnormalities resulting from lithium intoxication. *Angiology* 1997; **48:** 351–354.
10. Plielo E, Coelho A, Wetveer D. Persistent sinus node dysfunction secondary to lithium therapy. *Am Heart J* 1983; **106:** 1443–1444.
11. Arita M, Mashiba H. Effects of phenothiazine and propranolol on ECG. *Jpn Circ J* 1970; **34:** 391–340.
12. Ide A, Kamijo Y. Intermittent complete atrioventricular block after long term low-dose carbamazepine therapy with a serum concentration less than the therapeutic level. *Intern Med* 2007; **46:** 627–629.

Targeted Deletion of Class A Macrophage Scavenger Receptor Increases the Risk of Cardiac Rupture After Experimental Myocardial Infarction

Kenichi Tsujita, MD; Koichi Kaikita, MD; Takanori Hayasaki, MD; Tsuyoshi Honda, MD; Hironori Kobayashi, MD; Naomi Sakashita, MD; Hiroshi Suzuki, PhD; Tatsuhiko Kodama, MD; Hisao Ogawa, MD; Motohiro Takeya, MD

Background—Class A macrophage scavenger receptor (SR-A) is a macrophage-restricted multifunctional molecule that optimizes the inflammatory response by modulation of the activity of inflammatory cytokines. This study was conducted with SR-A–deficient ($SR\text{-}A^{-/-}$) mice to evaluate the relationship between SR-A and cardiac remodeling after myocardial infarction.

Methods and Results—Experimental myocardial infarction (MI) was produced by ligation of the left coronary artery in $SR\text{-}A^{-/-}$ and wild-type (WT) male mice. The number of mice that died within 4 weeks after MI was significantly greater in $SR\text{-}A^{-/-}$ mice than in WT mice ($P=0.03$). Importantly, death caused by cardiac rupture within 1 week after MI was 31% (17 of 54 mice) in $SR\text{-}A^{-/-}$ mice and 12% (6 of 51 mice) in WT mice ($P=0.01$). In situ zymography demonstrated augmented gelatinolytic activity in the infarcted myocardium in $SR\text{-}A^{-/-}$ mice compared with WT mice. Real-time reverse transcription–polymerase chain reaction at day 3 after MI showed that the expression of matrix metalloproteinase-9 mRNA increased significantly in the infarcted myocardium in $SR\text{-}A^{-/-}$ mice compared with WT mice. Furthermore, $SR\text{-}A^{-/-}$ mice showed augmented expression of tumor necrosis factor-α and reduction of interleukin-10 in the infarcted myocardium at day 3 after MI. In vitro experiments also demonstrated increased tumor necrosis factor-α and decreased interleukin-10 expression in activated $SR\text{-}A^{-/-}$ macrophages.

Conclusions—The present findings suggest that SR-A deficiency might cause impairment of infarct remodeling that results in cardiac rupture via insufficient production of interleukin-10 and enhanced expression of tumor necrosis factor-α and of matrix metalloproteinase-9. SR-A might contribute to the prevention of cardiac rupture after MI. (***Circulation***. **2007; 115:&NA;-.)**

Key Words: cytokines ■ macrophages ■ myocardial infarction ■ receptors ■ remodeling

Myocardial infarction (MI) causes complex structural alterations that involve both the infarcted and noninfarcted left ventricular (LV) myocardium.[1] The dynamic synthesis and breakdown of extracellular matrix (ECM) proteins play an important role in the post-MI LV remodeling,[2] which is a compensatory mechanism against LV dysfunction. However, the excessive degradation of ECM components in the infarcted regions appears to lead to pathological cardiac remodeling, which results in LV rupture.[3]

LV rupture is a lethal complication that accounts for 5% to 30% of in-hospital mortality in patients with acute MI and is most likely to occur during the first week after the onset of symptoms.[4] In addition, it is difficult to predict LV rupture in spite of the management of several risk factors such as transmural MI, a first MI, and hypertension. Recent studies have demonstrated that members of the matrix metalloproteinase (MMP) gene family play a central role in the degradation of ECM after MI.[5–7] Therefore, MMPs appear to play a major role in post-MI LV rupture. Furthermore, it has been shown that a key component of LV healing and remodeling after MI is the inflammatory response triggered by a wide variety of chemoattractants and inflammatory cytokines, which can modulate post-MI LV tissue repair.[8,9] We and others have reported that macrophage infiltration into the infarcted myocardium accelerated LV remodeling via increased activity of MMPs, which indicates macrophages that infiltrate into the infarcted regions are important contributors to the modulation of LV remodeling after MI.[10–12]

Clinical Perspective p 0000

Received June 13, 2006; accepted February 2, 2007.

From the Departments of Cell Pathology (K.T., T. Honda, H.K., N.S., M.T.) and Cardiovascular Medicine (K.T., K.K., T. Hayasaki, H.O.), Graduate School of Medical Sciences, Kumamoto University, Kumamoto, Japan; National Research Center for Protozoan Disease (H.S.), Obihiro University of Agriculture and Veterinary Medicine, Obihiro, Japan; and Department of Molecular Biology and Medicine (T.K.), Research Center for Advanced Science and Technology, University of Tokyo, Tokyo, Japan.

Correspondence to Koichi Kaikita, MD, Department of Cardiovascular Medicine, Graduate School of Medical Sciences, Kumamoto University, 1-1-1 Honjo, Kumamoto 860-8556, Japan. E-mail kaikitak@kaiju.medic.kumamoto-u.ac.jp

Circulation **is available at http://www.circulationaha.org** **DOI: 10.1161/CIRCULATIONAHA.106.671198**

Class A macrophage scavenger receptor (SR-A) is the prototypic member of an expanding family of membrane receptors collectively termed scavenger receptors. SR-A is also a macrophage-restricted multifunctional molecule.[13–15] SR-A can bind with high affinity to an unusually broad range of polyanionic ligands, which includes modified lipoproteins, lipopolysaccharide of Gram-negative bacteria, lipoteichoic acid of Gram-positive species, β-amyloid, and advanced glycation end products. On the basis of this broad ligand specificity, SR-A may play a role in a wide range of macrophage-associated physiological and pathophysiological processes.[16] Previous studies reported that SR-A was associated with the modification of atherosclerosis, macrophage adhesion, host defense, clearance of dying cells, and nervous system disorders. Moreover, Cotena et al recently showed that SR-A could ensure an inflammatory response of the appropriate magnitude via modulation of the activities of proinflammatory receptors and the production of several chemokines.[17] This suggests that SR-A might regulate inflammation itself and consequent tissue remodeling via macrophage function in the pathological conditions such as MI. However, there is no evidence that shows the involvement of SR-A in LV remodeling after MI. In the current paper, we report that a deficiency in the SR-A gene (SR-A$^{-/-}$) contributes to the risk of cardiac rupture after experimental MI via the modification of inflammatory cytokines and MMP expression.

Methods

Animals

Mice with targeted disruption of the SR-A gene (SR-A$^{-/-}$),[18] which is essential for the formation of SR-A, were used after at least the 8th backcross into the control C57BL/6J strain was reached.[19] Genotyping of animals was performed by use of polymerase chain reaction (PCR) of DNA obtained from tail biopsies. Recipient C57BL/6J mice and wild-type (WT) mice of the same genetic background were originally purchased from the Jackson Laboratory (Bar Harbor, Me). SR-A$^{-/-}$ and WT male mice were bred at the Animal Resource Facility at the Kumamoto University under specific pathogen-free conditions. All animal procedures were approved by the Animal Research Committee at Kumamoto University, and all procedures conformed to the *Guide for the Care and Use of Laboratory Animals* by the Institute of Laboratory Animal Resources. The SR-A$^{-/-}$ and WT mice were fed a regular chow diet and were used for experiments between 8 and 12 weeks of age.

Left Coronary Ligation

Mice were anesthetized with pentobarbital sodium (70 mg/kg) via intraperitoneal injection, and MI was induced by permanent occlusion of the left anterior descending coronary artery with an 8-0 Prolene suture under artificial ventilation, as previously described by our laboratory.[10] Significant electrocardiographic and color changes in the ischemic area were considered indicative of successful coronary occlusion. In the sham experiments, the same surgical procedure was performed, with the exception of coronary ligation.

Survival Rate

To evaluate survival after MI, the operation and autopsy were performed by a group of investigators who were blinded to the results of the genotyping. SR-A$^{-/-}$ and WT mice underwent coronary artery ligation and were monitored rigorously for morbidity and mortality. Autopsy was immediately performed in each animal after death to determine the cause of death, particularly with reference to cardiac rupture.

Echocardiography and Organ Weight Measurement for Assessment of LV Function

Echocardiographic measurements at baseline and on days 7 and 28 after surgery were performed with a Sonos 4500 with a high-frequency transducer (12 MHz; Philips Co., Tokyo, Japan) as previously described.[10,20] Good 2-dimensional views of the LV were obtained for guided M-mode measurements of interventricular septal wall thickness (IVS), posterior wall thickness (PW), LV end-diastolic diameter (LVDd), and end-systolic diameter (LVDs) as surrogate markers of LV dilatation caused by LV remodeling. M-mode percent fractional shortening (%FS) and LV mass were calculated by the following formulas:

$$(1)\qquad \%FS=\frac{LVDd-LVDs}{LVDd}\times 100$$

and

$$(2)\qquad \text{LV mass}=1.055\times[(IVS+PW+LVDd)^3-LVDd^3]\times 10^3,$$

respectively.[21] After in vivo echocardiographic studies at day 7 post-MI, the heart and lung were excised and their weights were determined. Moreover, the lungs were used to determine water content as a marker of lung congestion by calculation of the wet-to-dry ratio after desiccation for 24 hours at 50°C.[22]

Light Microscopy and Morphometric Analysis

At days 1, 3, 5 and 7 after coronary ligation, mice were euthanized for gross and microscopic cardiac analysis, with 6 to 10 animals studied at each time point. Heart tissues were fixed in 4% paraformaldehyde solution at 4°C for 4 hours, embedded in OCT compound (Sakura Finetechnical Co., Tokyo, Japan), frozen in liquid nitrogen, and cut by a cryostat into sections 6 μm thick. Sections were routinely stained with hematoxylin and eosin for light microscopy and with Masson's trichrome for evaluation of myocardial fibrosis. Infarct size and infarct area were determined by a previously reported method.[10] In brief, infarct size (%) was calculated as the total infarct circumference divided by the total LV circumference times 100; infarct area was calculated as the percentage of MI area relative to the entire LV tissue area.

Immunohistochemistry

Immunohistochemistry was performed according to an indirect immunoperoxidase method with the following antibodies: anti-CD204 for SR-A (2F8; Serotec, Oxford, UK); anti-CD68 for macrophages (FA-11; Serotec); anti-Ly-6G for granulocytes (Gr-1; Southern Biotechnology, Birmingham, Ala); anti-CD31 for endothelial cells (MEC13.3; Pharmingen, San Diego, Calif); anti–smooth muscle α-actin for myofibroblasts (1A4; Dako, Glostrup, Denmark). After inhibition of endogenous peroxidase activity by the method of Isobe et al,[23] the sections were incubated with the monoclonal antibodies described above at 4°C overnight. Goat anti-rat Ig-conjugated peroxidase-labeled polymer amino acid (Nichirei, Tokyo, Japan) was used as the secondary antibody. After visualization with 3,3′-diaminobenzidine, sections were stained with hematoxylin for nuclear staining and were mounted with resin. As negative controls, the same procedures were performed but without the primary antibodies. For cell enumeration, the number of positive cells in the infarcted region for each antibody was counted and expressed as the number per mm^2.

Detection of Gelatinolytic Activity by In Situ Zymography

To detect gelatinolytic activity in the infarcted heart tissues, we performed in situ zymography by use of a previously reported approach.[10] Gelatin films with sections were incubated for 6 hours at 37°C in a moisture chamber and stained with Biebrich Scarlet solution (Wako, Osaka, Japan). The gelatin in contact with the proteolytic areas of the sections was digested, which demonstrated zones of enzymatic activity indicated by negative staining.

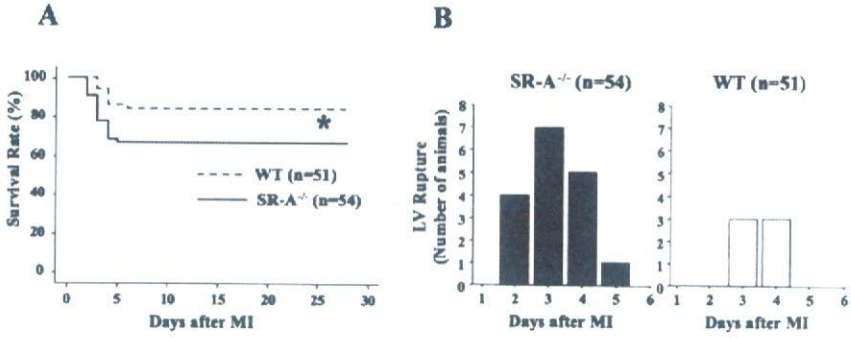

Figure 1. A, Survival of SR-A$^{-/-}$ and WT mice after MI. Survival curves are plotted for both SR-A$^{-/-}$ mice (n=54) and WT mice (n=51) as determined with the Kaplan-Meier method. *Log-rank P=0.027. B, Number of mice with cardiac rupture in SR-A$^{-/-}$ (17 of 54 mice) and WT (6 of 51 mice) mice within 1 week post-MI.

Real-Time Reverse Transcriptase-PCR Assay

Total RNA from heart tissues at day 3 after MI was extracted by the RNAzol B method (Tel-Test Inc., Friendswood, Tex). Total RNA was reverse-transcribed into cDNA using random primers (Life Technologies Inc., Rockville, Md). For detection of MMP-2, MMP-9, tissue inhibitor of metalloproteinase-1 (TIMP-1), TIMP-4, tumor necrosis factor-α (TNF-α), interleukin-1β (IL-1β), IL-10 and transforming growth factor-β (TGF-β) mRNA levels in heart tissue, real-time reverse transcriptase PCR was performed with an Applied Biosystems 7300 Real-time PCR System with TaqMan Universal PCR Master Mix and TaqMan Gene Expression Assays (Applied Biosystems, Foster City, Calif). Ribosomal eukaryotic 18S RNA (Applied Biosystems) was used as an endogenous control gene. A standard curve for the serial dilution of murine heart cDNA was generated. The amplification cycle consisted of 2 minutes at 50°C, 10 minutes at 95°C, 15 seconds at 95°C, and 1 minute at 60°C. The mRNA levels were normalized to the endogenous 18S ribosomal RNA gene expression.

In Vitro Assay of Cell Culture of Peritoneal Macrophages

To clarify the role of SR-A in the alteration of cytokine production in macrophages, we employed an in vitro assay system of peritoneal macrophages. Peritoneal macrophages were collected and suspended in RPMI 1640 medium (Sigma, St. Louis, Mo) that was supplemented with 10% fetal calf serum, 0.1 mg/mL streptomycin, and 100 U/mL penicillin, and then sowed at the density of 1.0×10^6/well on a plastic 24-well plate (Corning, Inc, Corning, NY).[24] The multiwell plate was incubated for 2 hours at 37°C in a humidified incubator with 5% CO_2. Each well was washed 10 times with 1 mL of PBS to remove nonadherent cells and was assigned either to receive acetylated low-density lipoprotein as a ligand for SR-A or not. Adherent macrophages were additionally cultured for 6 hours or 12 hours, and the supernatant was collected to determine the levels of TNF-α and IL-10 with sandwich ELISA. The assay was performed with commercially available mouse TNF-α ELISA kit (BioSource International, Camarillo, Calif) and mouse IL-10 Quantikine kit (R&D Systems, Minneapolis, Minn). Furthermore, to determine the inhibitory effects of recombinant mouse IL-10 (rmIL-10; R&D Systems) on TNF-α production of activated macrophages, we incubated peritoneal macrophages from both SR-A$^{-/-}$ and WT mice with 50 ng/mL and 200 ng/mL of rmIL-10 simultaneously with acetyl–low-density lipoprotein, a ligand for SR-A.

Statistical Analysis

Data are expressed as mean±2 SEM. Analyses of survival after MI were carried out by the Kaplan-Meier method with the log-rank test to compare survival curves between groups. Group comparisons were made with χ^2 tests for nominal data, and unpaired t tests or Mann-Whitney U tests were used for continuous data. Results with $P<0.05$ were considered statistically significant.

The authors had full access to and take full responsibility for the integrity of the data. All authors have read and agree to the manuscript as written.

Results

Survival and Cardiac Rupture after MI

The post-MI survival rates of SR-A$^{-/-}$ and WT mice were compared. There were no deaths in the sham-operated groups. As shown in Figure 1A, WT mice (84%, 43 of 51 mice) had significantly better survival after MI compared with SR-A$^{-/-}$ mice (67%, 36 of 54 mice). Interestingly, the most frequent cause of death in both SR-A$^{-/-}$ (17 of 18 mice) and WT (6 of 8 mice) mice was LV rupture, which was confirmed by blood coagulation around the pericardial sac and small slits commonly observed in the LV wall. As shown in Figure 1B, the number of the mice that died of LV rupture, which occurred within 5 days, was significantly greater in SR-A$^{-/-}$ mice (31%, 17 of 54 mice) than in WT mice (12%, 6 of 51 mice; P=0.01). During the experiments, no mice in either group were observed to have died from infectious diseases.

Physiological and Echocardiographic Measurement

As shown in Table 1, there were no significant differences in body weight, LVDd, M-mode %FS, LV mass at baseline or at days 7 and 28 post-MI between the 2 groups. Body weight, LVDd, and LV mass increased, and M-mode %FS decreased in both SR-A$^{-/-}$ and WT mice at days 7 and 28 post-MI. However, there were no significant differences between the 2 groups. Interestingly, relative heart weight (heart weight/body weight), relative lung weight (lung weight/body weight) and lung wet-to-dry ratio increased significantly in SR-A$^{-/-}$ mice compared with WT mice at day 7 post-MI.

Histomorphometric and Immunohistochemical Analysis

To evaluate the role of SR-A in the extent of ischemic damage in the infarcted myocardium, infarct size and infarct area were measured at day 7 post-MI. Histological analysis demonstrated that sham-operated myocardium had no signs of myocardial degeneration such as necrosis, fibrosis, hypertrophic change, or inflammatory response. As shown in Table 1, infarct size and area were nearly identical between the 2 groups (54.6±4.9% and 41.8±5.5%, respectively, for SR-A$^{-/-}$ versus 53.5±4.0% and 43.1±3.9%, respectively, for WT). Immunohistochemical analysis revealed the gradual infiltration of FA-11–positive macrophages into the infarcted region, which peaked at day 5 post-MI (Figure 2B). The accumulation of Gr-1–positive granulocytes into the infarcted region increased earlier, peaked at day 3 after MI, and gradually decreased in both groups (Figure 2C). The

General Characteristics of SR-A$^{-/-}$ and WT Mice

Parameter	Phase	SR-A$^{-/-}$	WT
BW, g	Baseline	22.5±1.2	22.0±0.2
	Day 7 after MI	23.6±1.1	23.8±1.0
	Day 28 after MI	26.2±1.2	26.8±0.7
Echocardiographic measurement			
LVDd, mm	Baseline	2.70±0.08	2.66±0.17
	Day 7 after MI	3.26±0.22	3.27±0.23
	Day 28 after MI	4.92±0.32	5.08±0.27
M-mode, %FS	Baseline	38.4±3.8	38.0±3.3
	Day 7 after MI	29.9±2.0	29.5±2.2
	Day 28 after MI	27.1±1.8	24.7±2.3
LV mass/BW	Baseline	3.55±0.29	3.15±0.37
	Day 7 after MI	6.69±0.70	6.15±0.67
	Day 28 after MI	6.38±0.69	6.02±0.72
Heart and lung weights			
Heart weight/BW, mg/g	Day 7 after MI	7.92±0.42*	6.27±0.56
Lung weight/BW, mg/g	Day 7 after MI	6.38±0.64*	5.34±0.30
Lung W/D weight ratio	Day 7 after MI	4.42±0.29*	4.04±0.11
Histomorphometric measurement			
Infarct size, %	Day 7 after MI	54.6±4.9	53.5±4.0
Infarct area, %	Day 7 after MI	41.8±5.5	43.1±3.9

BW indicates body weight; LVDd, left ventricular end-diastolic diameter; %FS, percent fractional shortening; and W/D, wet-to-dry.
*$P<0.05$ vs WT mice.

temporal change in infiltration of these inflammatory cells was identical between the 2 groups. In addition, immunostaining for CD31 and anti–smooth muscle α-actin revealed a similar presence of new blood vessels and myofibroblasts in the infarcted region of both groups (Figure 2A). SR-A–positive cells gradually appeared in the infarcted region of WT mice, although these cells were not observed in the preinfarcted heart tissues from both groups. The spatial and temporal SR-A expression corresponded to that of FA-11–positive macrophages. SR-A$^{-/-}$ mice were not immunopositive for the SR-A antibody at all, in contrast to WT mice (Figure 2A).

Masson's trichrome staining showed impaired healing of the infarcted myocardial tissue in SR-A$^{-/-}$ mice. That is, as shown in Figure 3A and 3C, there were loosely distributed collagen fibers and the retention of unprocessed necrotic myocardium in the infarcted region in SR-A$^{-/-}$ mice at day 7 post-MI. Conversely, as shown in Figure 3B and 3D, there was dense fibrosis in the entire infarcted region in WT mice.

MMP Expression and Activation in Infarcted Region

To evaluate the expression of MMPs and TIMPs, which play an important role in cardiac rupture after MI, we quantified cardiac MMP-2, MMP-9, TIMP-1, and TIMP-4 mRNA levels in SR-A$^{-/-}$ and WT mice. As shown in Figure 4A, the expression of MMP-9 mRNA increased significantly in the infarcted region compared with the noninfarcted or sham-operated myocardial tissues at day 3 post-MI in both SR-A$^{-/-}$ and WT mice, and was greater in the infarcted region of SR-A$^{-/-}$ mice than in that of WT mice. TIMP-1 mRNA expression also increased significantly in the infarcted region compared with the noninfarcted or sham-operated myocardial tissues at day 3 post-MI in both groups, and was inhibited more strongly in the infarcted region of SR-A$^{-/-}$ mice than WT mice. On the other hand, there was no significant difference in MMP-2 and TIMP-4 mRNA expression in the infarcted region between the SR-A$^{-/-}$ and WT mice, although MMP-2 mRNA was upregulated, and TIMP-4 mRNA

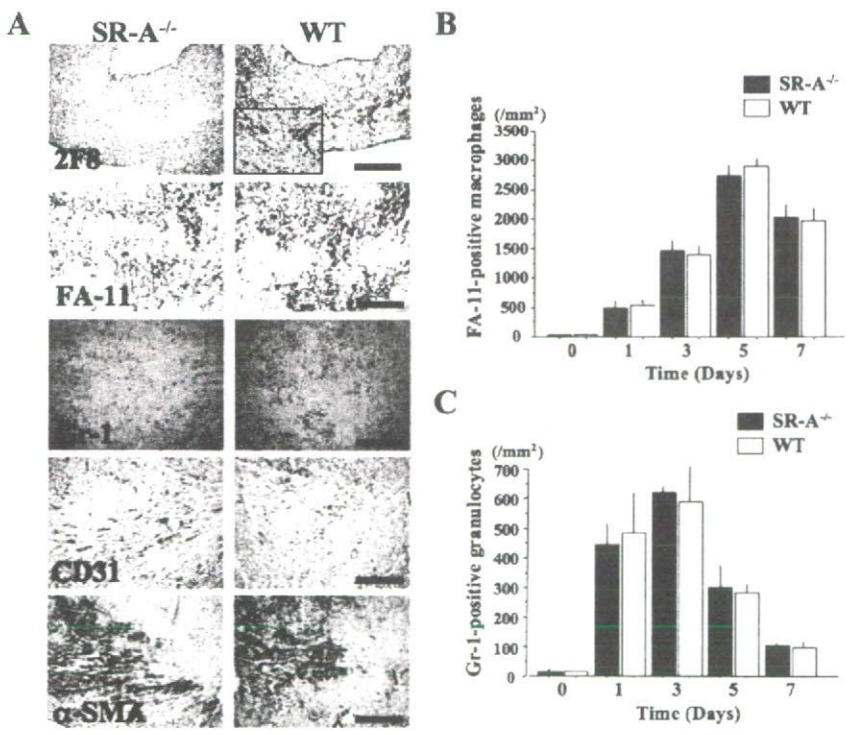

Figure 2. A, Immunohistochemical analysis of SR-A expression (2F8) and appearance of macrophages (FA-11), granulocytes (Gr-1), endothelial cells (CD31), and myofibroblasts (α-SMA) in infarcted regions of SR-A$^{-/-}$ (left) and WT (right) mice at day 3 post-MI. Scale bars represent 300 μm in each row. Cell enumeration of FA-11–positive macrophages (B) and Gr-1–positive granulocytes (C) in infarcted regions of SR-A$^{-/-}$ and WT mice at day 0, 1, 3, 5, and 7 post-MI. Data points represent the number of positive cells per mm^2. Bars represent mean±2 SEM.

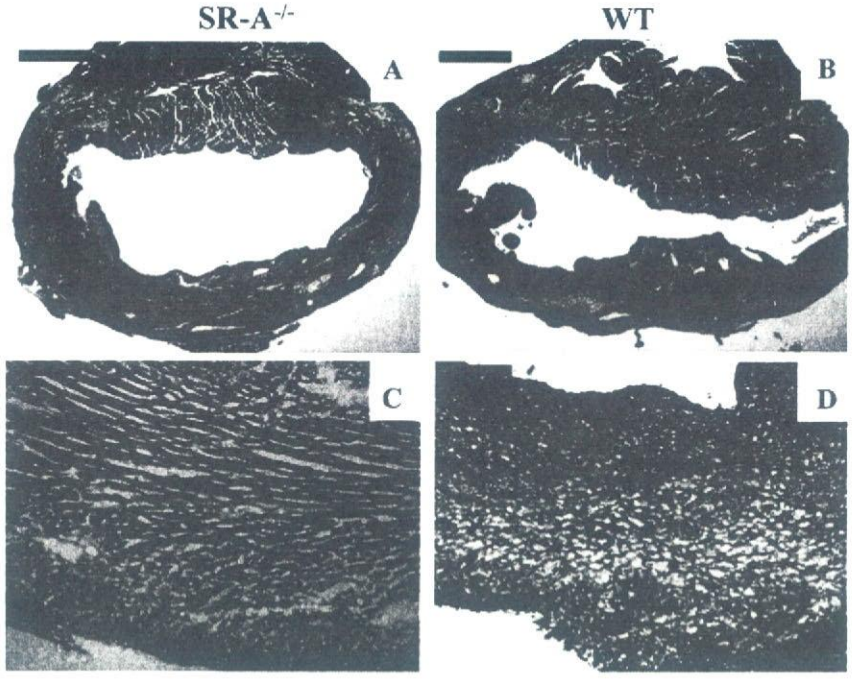

Figure 3. Representative low-power (A and B) and high-power (C and D) microphotographs of LV cross-sections stained with Masson's trichrome from SR-A$^{-/-}$ (A and C) and WT (B and D) mice at day 7 post-MI. Scale bars represent 1 mm in A and B and 200 μm in C and D.

was downregulated in the infarcted region compared with the noninfarcted or sham-operated myocardial tissues at day 3 post-MI in both SR-A$^{-/-}$ and WT mice.

We performed in situ zymography with gelatin films to detect gelatinolytic activity derived from the augmented MMP-9 mRNA expression in infarcted myocardial tissue. No gelatinolytic activity was detected at 1 day post-MI in either group (data not shown). In situ zymography demonstrated greater gelatinolytic activity in the infarcted region of SR-A$^{-/-}$ mice than WT mice at day 5 post-MI (Figure 4B). Moreover, morphometrically quantitative analysis of the gelatinolytic area/infarct area at day 5 post-MI confirmed the increased gelatinolytic activity in SR-A$^{-/-}$ mice (Figure 4C).

Expression of Inflammatory Cytokines

To examine the molecular mechanism that underlies the increased MMP activity in SR-A$^{-/-}$ mice, we determined cardiac mRNA expression of several cytokines and growth factors by real-time reverse transcriptase PCR. Interestingly, the proinflammatory cytokine TNF-α mRNA was upregulated in the infarcted region compared with the noninfarcted or sham-operated myocardial tissues at day 3 post-MI in both SR-A$^{-/-}$ and WT mice, and was greater in the infarcted region of SR-A$^{-/-}$ mice than WT mice (Figure 5A). The quantification of protein levels by ELISA also demonstrated upregulated TNF-α protein expression in the infarcted region of SR-A$^{-/-}$ mice (Figure 5E). In contrast, the antiinflammatory cytokine IL-10 mRNA was also upregulated in

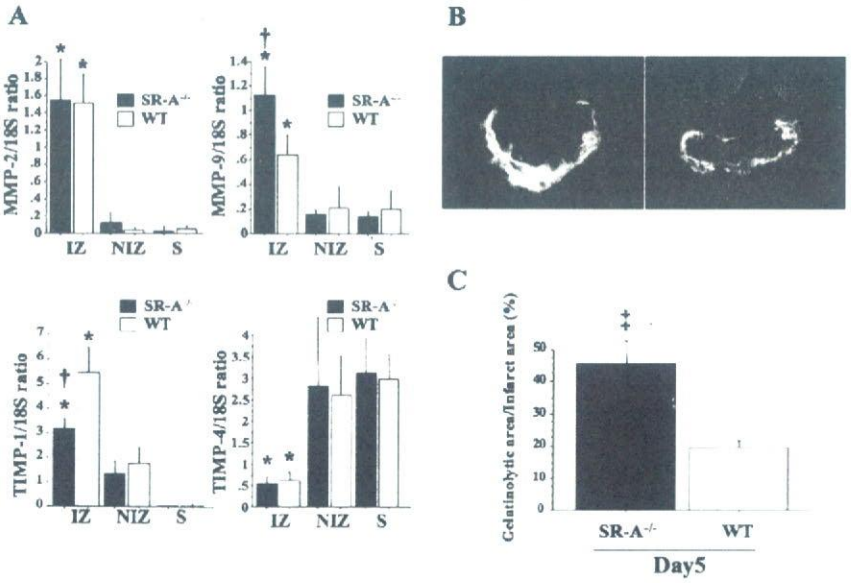

Figure 4. A, Real-time reverse transcriptase PCR results for MMP-2, MMP-9, TIMP-1, and TIMP-4 mRNA levels in infarcted zone (IZ), noninfarcted zone (NIZ), and sham-operated myocardium (S) from SR-A$^{-/-}$ and WT mice at day 3 post-MI. These mRNA levels were standardized by the levels of endogenous control 18S ribosomal RNA gene. Bars represent mean°2 SEM. *P<0.05 versus NIZ and S in each strain. †P<0.05 versus IZ in WT mice. B, In situ zymography in sections of infarcted myocardium from SR-A$^{-/-}$ (left) and WT (right) mice at day 5 post-MI. Lysis of gelatin in contact with the proteolytic areas of the sections is indicated by negative staining on the slides. C, Morphometric analysis of the gelatinolytic area/infarct area at day 5 post-MI in SR-A$^{-/-}$ and WT mice. Bars represent mean±2 SEM. ‡P<0.01 versus WT mice.

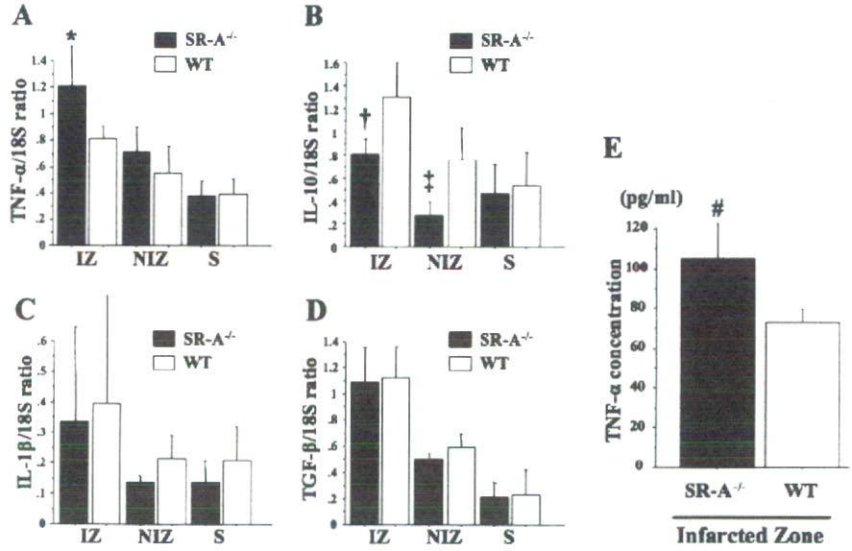

Figure 5. Real-time reverse transcriptase PCR for TNF-α (A), IL-10 (B), IL-1β (C), and TGF-β (D) mRNA levels in infarcted zone (IZ), noninfarcted zone (NIZ), and sham-operated myocardium (S) from SR-A$^{-/-}$ and WT mice at day 3 after MI. These mRNA levels were standardized by the levels of endogenous control 18S ribosomal RNA gene. Bars represent mean±2 SEM. *P<0.05 versus IZ in WT mice. †P<0.005 versus IZ in WT mice. ‡P<0.005 versus NIZ in WT mice. E, Quantification of TNF-α protein level by ELISA in infarcted region obtained from SR-A$^{-/-}$ and WT mice at day 3 after MI. Bars represent mean±2 SEM. #P<0.05 versus WT mice.

the infarcted region compared with the noninfarcted or sham-operated myocardial tissues at day 3 post-MI in both SR-A$^{-/-}$ and WT mice, and was significantly lower in the infarcted and noninfarcted region of SR-A$^{-/-}$ mice than WT mice (Figure 5B). Although other mRNAs of inflammatory cytokines and growth factors such as TGF-β, which appeared to regulate the synthesis and breakdown of ECM components, were also induced in the infarcted region compared with the noninfarcted region or sham-operated tissues, there were no significant differences between SR-A$^{-/-}$ and WT mice (Figure 5C and 5D).

In Vitro Analysis With Peritoneal Macrophages

We conducted in vitro experiments with peritoneal macrophages to confirm whether the imbalance in production of inflammatory cytokines detected in in vivo experiments could be reproduced in vitro. As shown in Figure 6A, IL-10 production increased significantly in both groups after 6 hours of incubation, but not after 12 hours. The levels of IL-10 production were significantly lower in SR-A$^{-/-}$ macrophages than WT macrophages when cultured with SR-A ligand for 6 hours, but not for 12 hours. As shown in Figure 6B, TNF-α production was significantly greater after 12 hours of incubation compared with production after 6 hours in both groups. The levels of TNF-α production were greater in SR-A$^{-/-}$ macrophages than WT macrophages when cultured with SR-A ligand for 12 hours, but not for 6 hours. With respect to the effects of rmIL-10 addition, the levels of TNF-α production by activated macrophages were significantly down-regulated in both SR-A$^{-/-}$ and WT macrophages after administration of 50 ng/mL rmIL-10, and the difference between both macrophages was diminished (Figure 6B). In contrast, in the group that received 200 ng/mL rmIL-10, the inhibitory effects on TNF-α production were absent (data not shown).

Discussion

Our study provided the first evidence that SR-A was essential for normal healing of infarcted myocardium. Specifically, we showed that SR-A$^{-/-}$ mice had a higher mortality mainly as a result of LV rupture after MI. The fragility of the LV wall in SR-A$^{-/-}$ mice might be attributable to markedly enhanced MMP activity in the infarcted myocardium. In the upstream mechanism, SR-A might be involved in the regulation of cytokine production and the ischemia-derived inflammatory response.

In the present study, we found that SR-A$^{-/-}$ mice had loosely distributed collagen fibers and retention of unprocessed necrotic myocardium in the infarcted region stained with Masson's trichrome. It has been demonstrated that MMPs might be the

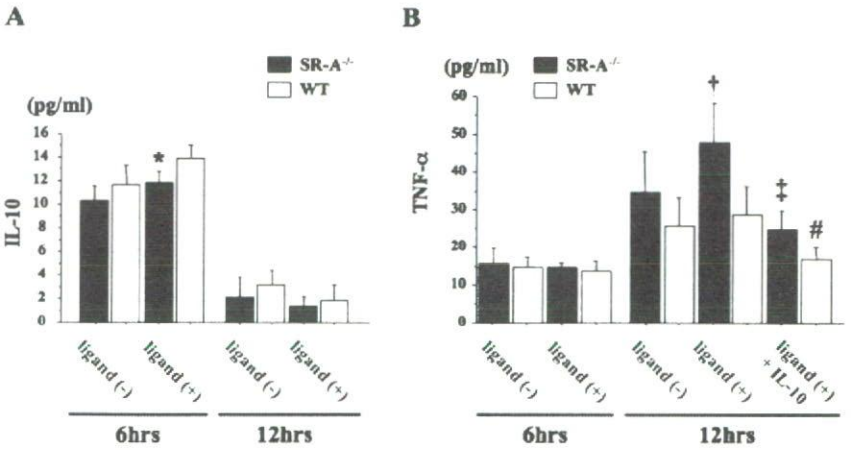

Figure 6. Quantification of IL-10 (A) and TNF-α (B) concentrations in culture medium of SR-A$^{-/-}$ and WT peritoneal macrophages in the presence or absence of SR-A ligand (acetyl-low-density lipoprotein). Bars represent mean±2 SEM. *P<0.05 versus WT macrophages incubated with SR-A ligand for 6 hours. †P<0.05 versus WT macrophages incubated with SR-A ligand for 12 hours. ‡P<0.01 versus SR-A$^{-/-}$ macrophages incubated with SR-A ligand for 12 hours without rmIL-10. #P<0.05 versus WT macrophages incubated with SR-A ligand for 12 hours without rmIL-10.

major pathophysiological regulators of ECM degradation and might be implicated in the pathogenesis of LV remodeling after MI.[5] Indeed, several studies in genetically-manipulated mice documented that gelatinases (ie, MMP-2 and MMP-9) play a crucial role in the LV remodeling process and may contribute to LV rupture.[6,7,25] Heymans et al demonstrated that MMP-9 deficiency prevented cardiac rupture after MI.[7] The significance of MMP-9 activity in early infarct healing and rupture was emphasized by the observation that MMP-9 was predominantly found in leukocytes and macrophages, and that its activity peaked around day 2, the period in which most ruptures occur. In the present study, quantitative reverse transcriptase PCR revealed increased MMP-9 mRNA expression and decreased TIMP-1 mRNA expression in the infarcted region of SR-A$^{-/-}$ mice at day 3 post-MI. In addition, in situ zymography indicated excessive gelatinolytic activity around the infarcted region of SR-A$^{-/-}$ mice. Taking these findings into consideration, enhanced gelatinolytic activity may directly contribute to the increased risk of post-MI LV rupture in SR-A$^{-/-}$ mice.

With regard to the upstream mechanism under the augmented MMP activity, Jugdutt reported that the net proteolytic activity of MMPs depended on transcription, activation, and inhibition of these molecules.[26] Transcription from MMP genes to pro-MMPs is stimulated by several factors such as inflammatory cytokines and growth factors.[27] Indeed, Sun et al recently showed that elevated local TNF-α in infarcted myocardium of TNF-α–deficient mice contributes to acute cardiac rupture via augmented MMP-9 expression.[28] TNF-α is a master proinflammatory cytokine that is produced in the infarcted myocardium very soon after MI and is potentially a major contributor to post-MI LV rupture.[28,29] On the other hand, antiinflammatory cytokines such as IL-10 are thought to have a protective role after MI through the suppression of the acute inflammatory process.[30–32] Very recently, Fulton et al demonstrated that SR-A$^{-/-}$ mice displayed reduced levels of lipopolysaccharide-induced IL-10 production, which regulated the inflammatory process in endotoxemia and sepsis.[33] Consistent with these findings, our data revealed that the expression of IL-10 mRNA was attenuated in the infarcted region of SR-A$^{-/-}$ mice compared with WT mice at day 3 post-MI. On the other hand, the expression of TNF-α mRNA increased significantly more in the infarcted region of SR-A$^{-/-}$ mice than in that of WT mice at day 3 post-MI. Moreover, we subsequently performed in vitro experiments with peritoneal macrophages to verify the contribution of SR-A to the imbalanced production of these proinflammatory and antiinflammatory cytokines. The present findings suggested that SR-A deficiency might enhance TNF-α secretion as a result of the suppression of IL-10 secretion in SR-A$^{-/-}$ macrophages. The imbalance of the production of inflammatory cytokines could be responsible for the markedly augmented MMP activity and increased risk of post-MI LV rupture. Furthermore, we showed the inhibitory effects of rmIL-10 administration on TNF-α secretion in the cell culture experiments. The more intense effect was observed in SR-A$^{-/-}$ macrophages. Therefore, SR-A–mediated IL-10 production may be a key step involved in the regulation of TNF-α production in activated macrophages.

In addition, organ weight analysis indicated that heart weight, lung weight, and lung wet-to-dry ratio increased significantly in SR-A$^{-/-}$ mice compared with WT mice at day 7 post-MI. These results suggested the exacerbation of post-MI myocardial hypertrophy or lung injury in SR-A$^{-/-}$ mice. The putative mechanisms for these findings include a direct effect of upregulated TNF-α on myocardial hypertrophy or lung congestion based on the adverse influence of TNF-α on post-MI heart and lung tissues.[28,34,35] In the present study, however, there was no significant difference in the echocardiographic measurements of LV cavity dimensions, M-mode %FS, and LV mass between the 2 groups. We must emphasize that echocardiographic measurements and histomorphological and biological analyses could only be performed in the surviving mice. It is possible that the degree of LV expansion, LV wall thinning, and LV dysfunction might have been greater in the mice that died as a result of early cardiac rupture and this may have biased the results. In addition, LV dimensions and function could have been greatly influenced by the stage of the anesthesia and hemodynamic parameters such as heart rate.[20] The reason why there were no significant differences in echocardiographic measurements between the 2 groups might have been caused by the exclusion of nonsurviving mice or hemodynamic changes as a result of anesthesia.

In summary, the present findings provide the first evidence of a pathophysiological role for SR-A in LV remodeling after MI and add further support for the importance of macrophages in the healing process after MI. Further research about the SR-A–related signaling pathway might provide innovative therapeutic approaches to prevent cardiac rupture after MI.

Acknowledgments

We thank Emi Kiyota, Takenobu Nakagawa, Osamu Nakamura, and Junichi Yoshida, from the Department of Cell Pathology, Kumamoto University, for their skillful technical assistance.

Sources of Funding

The present study was supported in part by a Grant from the Japan Heart Foundation and a Grant-in-Aid for Scientific Research (B-16390108, B-17390115, B-17390232, and C-17590752) from the Ministry of Education, Culture, Sports, Science, and Technology of Japan.

Disclosures

None.

References

1. Pfeffer JM, Pfeffer MA, Fletcher PJ, Braunwald E. Progressive ventricular remodeling in rat with myocardial infarction. *Am J Physiol*. 1991; 260:H1406–H1414.
2. Cleutjens JP, Kandala JC, Guarda E, Guntaka RV, Weber KT. Regulation of collagen degradation in the rat myocardium after infarction. *J Mol Cell Cardiol*. 1995;27:1281–1292.
3. Whittaker P, Boughner DR, Kloner RA. Role of collagen in acute myocardial infarct expansion. *Circulation*. 1991;84:2123–2134.
4. Antman EM, Braunwald E. Acute myocardial infarction. In: Braunwald E, Fauci AS, Kasper DL, Hauser SL, Longo DL, Jameson JL, eds. *Harrison's Principles of Internal Medicine*. 15th ed. New York: McGraw-Hill Book Co; 2001:1386–1399.
5. Creemers EE, Cleutjens JP, Smits JF, Daemen MJ. Matrix metalloproteinase inhibition after myocardial infarction: a new approach to prevent heart failure? *Circ Res*. 2001;89:201–210.
6. Hayashidani S, Tsutsui H, Ikeuchi M, Shiomi T, Matsusaka H, Kubota T, Imanaka-Yoshida K, Itoh T, Takeshita A. Targeted deletion of MMP-2 attenuates early LV rupture and late remodeling after experimental myocardial infarction. *Am J Physiol Heart Circ Physiol*. 2003;285:H1229–H1235.
7. Heymans S, Luttun A, Nuyens D, Theilmeier G, Creemers E, Moons L, Dyspersin GD, Cleutjens JP, Shipley M, Angellilo A, Levi M, Nube O, Baker A, Keshet E, Lupu F, Herbert JM, Smits JF, Shapiro SD, Baes M,

Borgers M, Collen D, Daemen MJ, Carmeliet P. Inhibition of plasminogen activators or matrix metalloproteinases prevents cardiac rupture but impairs therapeutic angiogenesis and causes cardiac failure. *Nat Med*. 1999;5:1135–1142.
8. Hawkins HK, Entman ML, Zhu JY, Youker KA, Berens K, Dore M, Smith CW. Acute inflammatory reaction after myocardial ischemic injury and reperfusion: development and use of a neutrophil-specific antibody. *Am J Pathol*. 1996;148:1957–1969.
9. Dreyer WJ, Michael LH, West MS, Smith CW, Rothlein R, Rossen RD, Anderson DC, Entman ML. Neutrophil accumulation in ischemic canine myocardium: insights into time course, distribution, and mechanism of localization during early reperfusion. *Circulation*. 1991;84:400–411.
10. Kaikita K, Hayasaki T, Okuma T, Kuziel WA, Ogawa H, Takeya M. Targeted deletion of CC chemokine receptor 2 attenuates left ventricular remodeling after experimental myocardial infarction. *Am J Pathol*. 2004; 165:439–447.
11. Hayashidani S, Tsutsui H, Shiomi T, Ikeuchi M, Matsusaka H, Suematsu N, Wen J, Egashira K, Takeshita A. Anti-monocyte chemoattractant protein-1 gene therapy attenuates left ventricular remodeling and failure after experimental myocardial infarction. *Circulation*. 2003;108:2134–2140.
12. Hayasaki T, Kaikita K, Okuma T, Yamamoto E, Kuziel WA, Ogawa H, Takeya M. CC chemokine receptor-2 deficiency attenuates oxidative stress and infarct size caused by myocardial ischemia-reperfusion in mice. *Circ J*. 2006;70:342–351.
13. Kodama T, Freeman M, Rohrer L, Zabrecky J, Matsudaira P, Krieger M. Type I macrophage scavenger receptor contains alpha-helical and collagen-like coiled coils. *Nature*. 1990;343:531–535.
14. Rohrer L, Freeman M, Kodama T, Penman M, Krieger M. Coiled-coil fibrous domains mediate ligand binding by macrophage scavenger receptor type II. *Nature*. 1990;343:570–572.
15. Freeman M, Ashkenas J, Rees DJ, Kingsley DM, Copeland NG, Jenkins NA, Krieger M. An ancient, highly conserved family of cysteine-rich protein domains revealed by cloning type I and type II murine macrophage scavenger receptors. *Proc Natl Acad Sci U S A*. 1990;87: 8810–8814.
16. Platt N, Haworth R, Darley L, Gordon S. The many roles of the class A macrophage scavenger receptor. *Int Rev Cytol*. 2002;212:1–40.
17. Cotena A, Gordon S, Platt N. The class A macrophage scavenger receptor attenuates CXC chemokine production and the early infiltration of neutrophils in sterile peritonitis. *J Immunol*. 2004;173:6427–6432.
18. Suzuki H, Kurihara Y, Takeya M, Kamada N, Kataoka M, Jishage K, Ueda O, Sakaguchi H, Higashi T, Suzuki T, Takashima Y, Kawabe Y, Cynshi O, Wada Y, Honda M, Kurihara H, Aburatani H, Doi T, Matsumoto A, Azuma S, Noda T, Toyoda Y, Itakura H, Yazaki Y, Horiuchi S, Takahashi K, Kruijt J, van Berckel T, Steinbrecher U, Ishibashi S, Maeda N, Gordon S, Kodama T. A role for macrophage scavenger receptors in atherosclerosis and susceptibility to infection. *Nature*. 1997;386:292–296.
19. Kamada N, Kodama T, Suzuki H. Macrophage scavenger receptor (SR-A I/II) deficiency reduced diet-induced atherosclerosis in C57BL/6J mice. *J Atheroscler Thromb*. 2001;8:1–6.
20. Takuma S, Suehiro K, Cardinale C, Hozumi T, Yano H, Shimizu J, Mullis-Jansson S, Sciacca R, Wang J, Burkhoff D, Di Tullio MR, Homma S. Anesthetic inhibition in ischemic and nonischemic murine heart: comparison with conscious echocardiographic approach. *Am J Physiol Heart Circ Physiol*. 2001;280:H2364–H2370.
21. Pollick C, Hale SL, Kloner RA. Echocardiographic and cardiac Doppler assessment of mice. *J Am Soc Echocardiogr*. 1995;8:602–610.
22. Pearce ML, Yamashita J, Beazell J. Measurement of pulmonary edema. *Circ Res*. 1965;16:482–488.
23. Isobe Y, Nakane PK, Brown WR. Studies on translocation of immunoglobulins across intestinal epithelium: I: improvements in the peroxidase-labeled antibody method for application to study of human intestinal mucosa. *Acta Histochem Cytochem*. 1977;10:161–171.
24. Hakamata H, Miyazaki A, Sakai M, Suginohara Y, Sakamoto Y, Horiuchi S. Species difference in cholesteryl ester cycle and HDL-induced cholesterol efflux from macrophage foam cells. *Arterioscler Thromb Vasc Biol*. 1994;14:1860–1865.
25. Ducharme A, Frantz S, Aikawa M, Rabkin E, Lindsey M, Rohde LE, Schoen FJ, Kelly RA, Werb Z, Libby P, Lee RT. Targeted deletion of matrix metalloproteinase-9 attenuates left ventricular enlargement and collagen accumulation after experimental myocardial infarction. *J Clin Invest*. 2000;106:55–62.
26. Jugdutt BI. Remodeling of the myocardium and potential targets in the collagen degradation and synthesis pathways. *Curr Drug Targets Cardiovasc Haematol Disord*. 2003;3:1–30.
27. Mauviel A. Cytokine regulation of metalloproteinase gene expression. *J Cell Biochem*. 1993;53:288–295.
28. Sun M, Dawood F, Wen WH, Chen M, Dixon I, Kirshenbaum LA, Liu PP. Excessive tumor necrosis factor activation after infarction contributes to susceptibility of myocardial rupture and left ventricular dysfunction. *Circulation*. 2004;110:3221–3228.
29. Irwin MW, Mak S, Mann DL, Qu R, Penninger JM, Yan A, Dawood F, Wen WH, Shou Z, Liu P. Tissue expression and immunolocalization of tumor necrosis factor-alpha in postinfarction dysfunctional myocardium. *Circulation*. 1999;99:1492–1498.
30. Frangogiannis NG, Mendoza LH, Lindsey ML, Ballantyne CM, Michael LH, Smith CW, Entman ML. IL-10 is induced in the reperfused myocardium and may modulate the reaction to injury. *J Immunol*. 2000;165: 2798–2808.
31. Lacraz S, Nicod LP, Chicheportiche R, Welgus HG, Dayer JM. IL-10 inhibits metalloproteinase and stimulates TIMP-1 production in human mononuclear phagocytes. *J Clin Invest*. 1995;96:2304–2310.
32. Yang Z, Zingarelli B, Szabo C. Crucial role of endogenous interleukin-10 production in myocardial ischemia/reperfusion injury. *Circulation*. 2000; 101:1019–1026.
33. Fulton WB, Reeves RH, Takeya M, De Maio A. A quantitative trait loci analysis to map genes involved in lipopolysaccharide-induced inflammatory response: identification of macrophage scavenger receptor 1 as a candidate gene. *J Immunol*. 2006;176:3767–3773.
34. Sack MN, Smith RM, Opie LH. Tumor necrosis factor in myocardial hypertrophy and ischaemia–an anti-apoptotic perspective. *Cardiovasc Res*. 2000;45:688–695.
35. Bradham WS, Bozkurt B, Gunasinghe H, Mann D, Spinale FG. Tumor necrosis factor-alpha and myocardial remodeling in progression of heart failure: a current perspective. *Cardiovasc Res*. 2002;53:822–830.

CLINICAL PERSPECTIVE

Despite improved treatments for acute myocardial infarction (MI), post-MI cardiac rupture remains a serious acute complication. Unfortunately, cardiac rupture mainly develops in younger patients with a transmural MI and is also unpredictable and fatal because of the absence of treatment. Accumulated experimental and clinical studies have indicated that members of the matrix metalloproteinase gene family play a central role in pathogenesis of cardiac rupture. Furthermore, we believe that understanding inflammatory response is critical for the prevention of post-MI cardiac rupture because the matrix metalloproteinase activation may be regulated mainly by various inflammatory mediators. In the present study, we evaluated the role of class A macrophage scavenger receptor (SR-A), which was a macrophage-restricted multifunctional molecule that optimized the inflammatory response in post-MI tissue repair. Our data revealed that a deficiency in the SR-A gene increased the risk of cardiac rupture after experimental MI via enhanced matrix metalloproteinase expression in infarcted myocardium. Moreover, we observed that SR-A deficiency enhanced tumor necrosis factor-α secretion as a result of the suppression of interleukin-10 secretion in SR-A–deficient macrophages. These findings suggest that SR-A might regulate macrophage-associated inflammatory responses in infarcted regions and might modulate consequent tissue remodeling in the healing process after MI. Further research into the SR-A–related signaling pathway might provide innovative therapeutic approaches to prevent cardiac rupture.

研究

心不全例における カルベジロール導入クリティカルパスの有用性*

宮尾　雄治[1]　田中　朋子　福嶋隆一郎
原田　恵実　藤本　和輝

要旨　【目的】クリティカルパスは治療手技の標準化，入院期間の適正化に有用な手段とされる．心不全入院例でのパス使用下β遮断薬導入の有用性を検討する．【方法】カルベジロール導入を行った51例を，パス使用群22例(P群)とパス非使用群29例(C群)に分けた．両群間で入院期間，入院費用などを比較し，入院期間に関連する因子の検討を行った．【結果】P群にて，入院期間(20.2±9.7 vs 34.3±12.0，$p<0.0001$；P群 vs C群，Mean±SD)，カルベジロール開始後入院期間(12.8±3.6 vs 23.4±11.8，$p<0.0001$)は有意に短く，総入院費用(77,311±39,161 vs 110,693±52,742，$p<0.05$)は低い．最終カルベジロール用量(10.6±5.1 vs 9.6±4.4)には差はなかった．重回帰分析ではパスの有無のみが入院期間に関連する有意な説明因子であった．【結語】心不全患者へのカルベジロール導入パスは費用負担の軽減と入院期間の短縮に寄与する有用な手段である．

キーワード　クリティカルパス，心不全，カルベジロール

循環器疾患のなかでも心不全は多くの循環器疾患の終末像にあたる病態であり，直接生命予後に関連する疾患であるとともに，生活の質を著しく低下させるばかりでなく，長期にわたり入退院を繰り返す主たる原因となっている．欧米を中心とした大規模臨床試験において，心不全の治療にβ遮断薬を使用することで予後を改善したり，心不全による再入院を減少させたりすることが証明された[1~3]．先頃示された本邦における慢性心不全治療ガイドライン[4]にても，β遮断薬はアンジオテンシン変換酵素阻害薬とともに無症候性(NYHA I)の段階から使用することを推奨されており，心不全患者には広く使用されるべき有用な薬剤である．しかしながら，心不全患者へのβ遮断薬の導入に際しては，少量よりゆっくりと増量する必要があり，症例ごとに主治医の裁量のもとに，増量のタイミングや入院期間の設定を行っていた．そのため，入院期間の長期化を招くという問題があり，これらのこともあるためか，本邦においてはいまだ十分に心不全患者にβ遮断薬が使用されるようになったとは言い難い．

クリティカルパスは，計画的に検査治療を行うことで無駄を省き，また看護師や薬剤師，栄養士などのチームアプローチによる患者教育を含む標準化された医療を行うことができ，治療手技の適切性を判断する手法となりうる．そこで今回われわれは，当院に心不全で入院した患者において，クリティカルパスを使用したカルベジロール導入治療の有効性と安全性について入院期間および医療経済的側面，パスバリアンスなどの点からの検討を行うこととした．

方　法

対象は，2001年9月から2007年3月の期間に心不全症状にて入院した患者のなかで，新規にカルベジロール導入を行った51例とした．基礎疾患や左室駆出率による基準は設けず，心不全の状態が改善し，主治医がβ遮断薬導入可能と判断した時点で，カルベジロールの導入開始とした．クリティカルパスを作成した2004年4月以後は，パスを使用してのカルベジ

* Effectiveness of the Critical Path for Administering Carvedilol in Patients with Congestive Heart Failure(2008年1月23日受付)

[1] 国立病院機構熊本医療センター循環器科(〒860-0008 熊本市二の丸1-5)　Yuji Miyao, Tomoko Tanaka, Ryuichirou Fukushima, Megumi Harada, Kazuteru Fujimoto：Department of Cardiology, National Hospital Organization Kumamoto Medical Center

0452-3458/08/¥500/論文/JCLS

表1 登録患者臨床背景

	C群(n=29)	P群(n=22)	p
年齢(歳)(Mean±SD)	64.8±14.2	65.9±14.3	N.S.
男性/女性(%)	76/24	82/18	N.S.
IHD/Non IHD(%)	14/86	36/64	N.S.
ACE-I or ARB(%)	97	95	N.S.
ACE-I+ARB(%)	10	5	N.S.
ジギタリス剤(%)	35	32	N.S.
利尿剤(%)	83	82	N.S.
DM/HT/HLP/SM(%)	41/59/14/21	23/45/45/18	N.S.
LVEF(%)	42.8±11.5	47.1±14.1	N.S.
LVDd(mm)	58.9±9.8	57.1±10.8	N.S.
LVDs(mm)	46.4±10.0	43.5±12.0	N.S.
収縮期血圧(mmHg)	126±26	122±38	N.S.
心拍数(rpm)	90.0±22.9	80.3±21.4	N.S.
BNP(pg/ml)	408±464	410±501	N.S.
院内死亡(%)	0	0	N.S.

IHD: ischemic heart disease, ACE-I: angiotensin converting enzyme inhibitor, ARB: angiotensin receptor blocker, DM: diabetes mellitus, HT: hypertension, HLP: hyperlipidemia, SM: smoking, LVEF: left ventricular ejection fraction, LVDd: left ventricular diastolic dimension, LVDs: left ventricular systolic dimension, BNP: B-type natriuretic peptide

ロールの導入を行い，それ以前は従来の方法である主治医の判断，裁量により検査予定や増量のタイミングを決定していくこととした．これにより51例は，パス使用群22例(男性18例，女性4例；平均年齢65.9±14.3歳)(P群)，パス非使用群29例(男性22例，女性7例；平均年齢64.8±14.2歳)(C群)に分けられた．利尿薬，ジギタリス薬，アンジオテンシン変換酵素阻害薬，アンジオテンシンII受容体拮抗薬などの既にその患者に使用中の心不全治療薬は基本的には続行とした．

カルベジロール導入クリティカルパスは，カルベジロール1.25 mgを1日2回投与(1日量2.5 mg)より開始し，3～7日(標準4日)ごとに認容性に問題なければ増量とし，1日10 mgまでの増量とするプロトコールとした．観察項目内に症状やバイタルサインなどの項目を設け，また採血や胸部X線写真などの定期的な検査を行い，心不全悪化や副作用などがないかチェックできるようにした．パス内には服薬指導や栄養指導，生活指導などが漏れないように設定した．カルベジロールの増量の是非については主治医の判断とした．C群においては，従来どおりの方法で，カルベジロールの増量のタイミングや検査施行に関しては主治医の判断で行った．

両群間において心機能・心不全指標〔入院時の収縮期血圧，心拍数，左室拡張終期径(LVDd)，左室収縮終期径(LVDs)，左室収縮係数，左室駆出分画率(LVEF)などの心臓超音波検査指標，血漿BNP濃度〕や血清クレアチニン値を比較するとともに，入院期間，カルベジロール導入後の入院期間および入院費用(出来高)に関して比較検討した．また，多変量解析手法を用いて，入院期間に有意に関連する因子の検討を行った．

■結　果

患者の臨床背景，服薬内容を表1に示す．両群間の年齢，男女比，虚血性心筋障害，糖尿病，高脂血症，高血圧，喫煙の有無に差はなく，また内服内容にてアンジオテンシン変換酵素阻害薬やアンジオテンシンII受容体拮抗薬などの使用率にも差がなかった．その他，心臓超音波指標，入院時収縮期血圧，脈拍値，症状安定期の退院前BNP値にも特に有意な差を認めなかった．患者ごとの入院期間を比較すると，P群では20.2±9.7日であり，これはC群の34.3±12.0日に比較し有意に短かった($p<0.0001$)．また，カルベジロール導入開始後の入院期間の比較においても，P群では12.8±3.6日であり，C群の23.4±11.8日に比較し有意に短かった($p<0.0001$)(図1)．

両群間のカルベジロールの最終投与量の比較では，P群では9.6±4.4 mg，C群では10.6±5.1 mgと両群の間には有意な差を認めなかった．

出来高ベースでの入院費用を両群間で比較すると，P群では77,311±39,161点であり，これはC群の110,693±52,742点に比較し有意に低かった($p<0.05$)．これをそれぞれの症例ごとに入院期間で除して，1日当たりの点数として比較すると，P群では3,897±778点であり，これはC群の3,259±1,127点に比較し有意に高かった($p<0.05$)．

入院期間に関連する因子を検討するため，年齢，性別，カルベジロールの用量，左室収縮率，LVDd，血清クレアチニン値，パス使用の有無を説明変数として重回帰分析を行った．この解析にては，パス使用の有無のみが有意な説明因子であった($p<0.0001$)(表2)．

P群におけるパスのバリアンスを調べてみると，全身倦怠感と血圧低下のため1例が脱落となった．パス逸脱と判断される例としては，1例が血圧低めとなり，パスどおりに増量できず，また2例は主治医の意向で投与量をカルベジロール20 mgまで引き続き増量した例であった．また，正のバリアンスと判断される例も4例あった．これは主に軽症例で患者が早期退院を希望した例であった．P群における脱落例と同様

にC群においても1例，カルベジロール増量に伴い心不全増悪となった症例があった．

考　察

心不全患者へのカルベジロール導入のためのクリティカルパスは，22例中1例にパス脱落例を認めるが，同じような合併症の発生はパスを使用しない場合にも認め，概ね合併症なくカルベジロールの導入と増量が可能であると思われた．カルベジロールを心不全患者に使用することで，生命予後および必要な医療費の抑制が可能であるとの報告[5,6]と心不全入院例の治療管理に対しクリティカルパスを使用することで，その有用性を示した報告[7]もある．今回，われわれの検討では，カルベジロール導入に際しクリティカルパスを使用することで，パスを使用しない従来どおりのカルベジロール導入法に比べ有意に入院期間を短縮させ，またこれにより総入院費用も有意に抑制することができた．このことは，医療政策，医療経済的視点からもパスを使用することは有用な手段の一つと言うことができる．

今回検討した対象症例はいずれも急性心不全もしくは慢性心不全増悪にて入院した症例で，急性期の治療を経て，心不全状態が改善した後にカルベジロールの導入開始とした．そのため総入院期間としては両群ともかなり長い状況となった．今後，外来の慢性心不全患者で心機能低下が著明であるために入院にてのβ遮断薬導入を必要とする患者に対して，上記クリティカルパスを使用してみることを検討したい．

β遮断薬の心不全患者に対する有効性は，先に示したように諸外国の大規模臨床試験[1~3]で示されてきた．しかし，人種的な違いもあってか，これら諸外国の適応用量は本邦での臨床使用用量よりかなり多いものである．今回の検討では，β遮断薬としてカルベジロールを選択し，その目標到達用量は10 mgとした．これは，本邦の臨床試験において，カルベジロールは少量であっても有効性を認めることが示されていること[8]，心不全治療薬として本邦で保険承認されているβ遮断薬で唯一の薬剤であることと，カルベジロールとメトプロロールの比較試験においてカルベジロールの有用性を示した報告[9]もあるため，このようなプロトコールとした．

今回のパスにおいてもバリアンス例を認めた．脱落となった1例はLVDdが93 mmで，LVEFが27%と非常に心機能の低下した重症例であった．また，正のバリアンスの例は，逆にLVEFも高く軽症例であった．これらの点をふまえて考えると，重症度に応じてカルベジロールの増量のタイミングの設定を変えたパスをいくつか作成することもバリアンスを少なくする点では有効と思われ，今後の課題としたい．

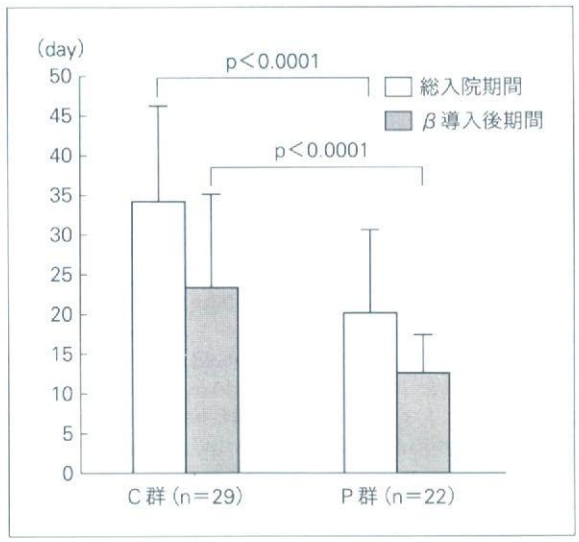

図1　パス使用群とパス非使用群での入院期間の比較

表2　重回帰分析による総入院期間に関連する因子の検討

	回帰係数	標準誤差	標準回帰係数	T値	p値
パスの有無	−14.4	3.22	−0.55	−4.48	p<0.0001
LVDd	−0.37	0.19	−0.28	−1.97	p=0.06
年齢	−0.18	0.13	−0.20	−1.39	N.S.
血清Cr	−2.81	4.26	−0.09	−0.66	N.S.
性別	0.53	4.15	0.02	0.13	N.S.
LVEF	−0.02	0.13	−0.03	−0.18	N.S.
カルベジロール用量	−0.001	0.35	−0.01	−0.003	N.S.

文　献

1) The Cardiac Insufficiency Bisoprolol Study II (CIBIS-II): a randomized trial. Lancet 353: 9-13, 1999
2) Packer M, Bristow MR, Cohn JN, et al: The effect of carvedilol on morbidity and mortality in patients with chronic heart failure. N Engl J Med 334: 1349-1355, 1996
3) Effect of metoprolol CR/XL in chronic heart failure: Metoprolol CR/XL Randomized Intervention Trial in Congestive Beart Failure(MERIT-HF). Lancet 353: 2001-2007, 1999
4) 循環器病の診断と治療に関するガイドライン(2004年度合同研究班報告)：慢性心不全治療ガイドライン(2005年改訂版), Guidelines for Treatment of Chronic Heart Failure(JCS 2005)

5) Inomata T, Izumi T, Kobayashi M: Cost-effectiveness analysis of carvedilol for the treatment of chronic heart failure in Japan. Circ J 68: 35-40, 2004
6) Stewart S, McMurray JJ, Hebborn A, et al: Carvedilol reduces the costs of medical care in severe heart failure: an economic analysis of the COPERNICUS study applied to the United Kingdom. Int J Cardiol 100: 143-149, 2005
7) Ranjan A, Tarigopula L, Srivastava RK, et al: Effectiveness of the clinical pathway in the management of congestive heart failure. South Med J 96: 661-663, 2003
8) Hori M, Sasayama S, Kitabatake A, et al; MUCHA Investigators: Low-dose carvedilol improves left ventricular function and reduces cardiovascular hospitalization in Japanese patients with chronic heart failure: the Multicenter Carvedilol Heart Failure Dose Assessment (MUCHA) trial. Am Heart J 147: 324-330, 2004
9) Poole-Wilson PA, Swedberg K, Cleland JG, et al; Carvedilol Or Metoprolol European Trial Investigators: Comparison of carvedilol and metoprolol on clinical outcomes in patients with chronic heart failure in the Carvedilol or Metprolol European Trial (COMET): randomized controlled trial. Lancet 362: 7-13, 2003

Summary

Effectiveness of the Critical Path for Administering Carvedilol in Patients with Congestive Heart Failure

by

Yuji Miyao, Tomoko Tanaka, Ryuichirou Fukushima, Megumi Harada, Kazuteru Fujimoto

from

Department of Cardiology, National Hospital Organization Kumamoto Medical Center

The critical path, which used a multidisciplinary team approach, included an intensive education program. The aim of this study was to evaluate the effect of administration of carvedilol critical path on length of stay and hospital cost. METHODS: We studied 51 patients at admission for CHF and started the carvedilol from September, 2001 to March, 2007. These patients were divided into the post-implementation of the critical path (Path group: P) (22 patients) and the pre-implementation of the critical path (Control group: C) (29 patients). The carvedilol was commerced, using the critical path for patients in the P group and using the traditional practice in the C group. The predictors of length of hospital stay were evaluated by multiple regression analysis. RESULTS: Baseline characteristics of the two groups were similar. The use of the path revealed significant decreases in length of hospital stay (20.2±9.7 vs. 34.3±12.0, $p<0.0001$), length of stay from starting carvedilol (12.8±3.6 vs. 23.4±11.8, $p<0.0001$), and hospital cost (77,311±39,161 vs. 110,693±52,742, $p<0.05$) in the P and C group, respectively. The use of the path was the only independent predictor of length of hospital stay. CONCLUSION: The critical path for administering carvedilol can decrease length of stay and hospital cost.

Key words critical path, heart failure, carvedilol